IOPscience iopscience.iop.org

Home Search Collections Journals About Contact us My IOPscience

Long-range migration of intrinsic defects during irradiation or implantation

This article has been downloaded from IOPscience. Please scroll down to see the full text article.

2009 J. Phys.: Condens. Matter 21 364219

(http://iopscience.iop.org/0953-8984/21/36/364219)

View the table of contents for this issue, or go to the journal homepage for more

Download details:
IP Address: 129.252.86.83
The article was downloaded on 30/05/2010 at 04:57

Please note that terms and conditions apply.

IOP PUBLISHING JOURNAL OF PHYSICS: CONDENSED MATTER
J. Phys.: Condens. Matter **21** (2009) 364219 (8pp) doi:10.1088/0953-8984/21/36/364219

Long-range migration of intrinsic defects during irradiation or implantation

J W Steeds, W Sullivan, A Wotherspoon and J M Hayes

Department of Physics, University of Bristol, Bristol BS8 1TL, UK

E-mail: j.w.steeds@bris.ac.uk

Received 5 April 2009
Published 19 August 2009
Online at stacks.iop.org/JPhysCM/21/364219

Abstract
A series of electron irradiations has been performed on diamond and 4H SiC single crystal specimens. A wide range of different doses and dose rates was investigated. In addition, a more limited investigation of localized hydrogen and helium implantation of 4H SiC has been made. The electron energies were sufficient to cause atomic displacements creating vacancies and self-interstitials in the irradiated samples. After electron-irradiation or implantation the samples were studied by low temperature (∼7 K) photoluminescence microscopy. It was found that some of the defect centres migrated over large distances outside of the irradiated regions and that this distance increased with increase of the dose. Two possible explanations for this remarkable behaviour are discussed. One is based on the absorption by the defects of light created by recombination of electrons and holes in the irradiated or implanted region. The other deals with the consequences of recombination-enhanced migration at point defects that traps carriers as they are driven out of the irradiated region by electric fields created during the irradiation or implantation process. Interstitial atoms are deduced as migrating further than vacancies in this process.

(Some figures in this article are in colour only in the electronic version)

1. Introduction

When we first studied, by low temperature photoluminescence microscopy, electron radiation damage created in chemical vapour deposited (CVD) diamond using a transmission electron microscope, it quickly became evident that conditions could be set up that caused certain radiation damage centres to migrate large distances (>50 μm) outside of the irradiated area [1]. Very similar results were subsequently found in electron-irradiated 4H SiC [2]. In fact there is a trail of earlier references that provide evidence of related observations in other materials. In 1967 Starodubtsev *et al* [3] reported radiation-stimulated migration of Cd over distances of 100 μm in CdS. Lima and Howie [4] found electron-irradiation damage of Ge propagating distances greater than 10 μm outside of the irradiated regions. There has been a succession of related observations of long distance propagation of O in electron-irradiated quartz starting in 1995 [5] with a detailed atomic mechanism proposed recently [6] with a calculated migration energy of 0.11–0.27 eV. More controversially, Popovici *et al* [7] reported the field-enhanced diffusion of B, O, N and Li into diamond over distances of at least 0.5 μm. Electron paramagnetic resonance investigations have also concluded that radiation-enhanced interstitial migration occurs in diamond at a temperature of 100 K [8].

In the present work we bring together results obtained from diamond and 4H SiC. Both these materials may be obtained with low levels of dopant and impurity and the understanding of the atomic nature of intrinsic defects in these materials after electron-irradiation and their mobilities is currently at a comparable level; they have wide band-gaps and either lack (diamond) or have relatively low (4H SiC) macroscopic Coulomb fields arising from their bulk longitudinal optic phonons. There are marked similarities in the results obtained. A major difference between them is the two atom basis of the SiC so that it has both Si and C vacancies and self-interstitials and antisite defects also occur. The results to be presented are quite general in nature over broad ranges of materials that are relatively pure and perfect within limits that will be discussed in the text. From a review of the experiments carried out it is concluded that the results are a consequence of several different aspects of radiation-enhanced migration.

 © 2009 IOP Publishing Ltd Printed in the UK

Table 1. Details of diamond samples studied. 1 ppm is approximately 2×10^{17} cm^{-3}.

Source	Type	N level	Comments
Butler	Polycrystal	<1 ppm	Weak Si-vacancy PL
DERA	Polycrystal	~1 ppm	Weak Si-vacancy PL
Natural IIA	Single crystal	~1 ppm	Defect banding
DTC	HPHT	<1 ppm	Growth sector, low dislocation density
DTC	HPHT	N/A	B-doped 2–8 ppm
Element 6	CVD single crystal	<10 ppb	Dislocations

Table 2. Details of SiC samples studied.

Source	Doping (cm^{-3})	Number studied	Epi-layer thickness (μm)
IKZ Berlin	N, 10^{13}–10^{15}	2	30
	Al, 10^{14}–10^{16}	8	30
Cree	N, 10^{14}–10^{16}	4	30
SiCrystal	Al, $\sim 10^{16}$	1	30
Linkoping	N, 10^{13}–10^{15}	4	30
ST Catania	N, 10^{13}–10^{14}	4	80

2. Experimental techniques

As reviewed elsewhere [1] the samples were irradiated in bulk form by electrons using an ion-free Philips EM430 transmission electron microscope (TEM) that was modified for ion-free operation. The TEM was operated at voltages in the range 150–300 kV with an electron beam of uniform intensity within a circular area with diameter varying from 10 to 200 μm and a rapid drop-off of intensity at the periphery. A wide range of doses and dose rates was investigated. All of the irradiations reported were performed at room temperature since previous work had indicated that cooling the sample to ~30 K during irradiation did not have a detectable effect on the results [1]. Of course, some heating will have occurred but any temperature rise was certainly below 250 °C for the SiC and 350 °C for the diamond because the irradiated samples were found to contain defect centres that are known to anneal out at these temperatures. 350 °C is well below the temperature at which C interstitials become mobile in diamond. Isolated C interstitials are mobile below room temperature in 4H SiC but, on warming a low temperature irradiated sample to room temperature, they form complexes that are stable to at least 350 °C. The similarity of the spectra obtained from both diamond and 4H SiC, for a given dose, from samples electron-irradiated at about 20 K to those from samples without cooling, probably indicates that the temperature rise was considerably lower than these upper limits. A few irradiations of both materials were performed at 600 and 800 kV using the high resolution JEOL TEM at the US National Center for Electron Microscopy in Berkeley, CA. The ion-implantation experiments were performed at the University of Surrey Ion Beam Centre on 30 μm thick, 2×10^{16} cm^{-3}, p(Al)-doped epilayers of 4H SiC. They were implanted with 1 MeV H and He ion beams focused to a diameter of about 5 μm to various doses in the range from 10^{18} to 5×10^{20} cm^{-2} without sample cooling. Details of the samples studied are summarized in tables 1 and 2.

After irradiation or implantation the samples were transferred to an Oxford Instruments Microstat cryogenic stage attached to one of two Renishaw micro-Raman spectrometers. One of these was operated with an HeCd laser at an excitation wavelength of 325 nm, the other was operated with an argon-ion laser using an excitation wavelength of 488 nm. Photoluminescence (PL) spectra were obtained at chosen points, at equally spaced points along a line through (and outside) the irradiated region (a 'line-scan') and at points in a rectangular (x, y) array covering the irradiated region and its periphery (a 'map'). All of the PL results presented here were obtained with liquid-helium cooling at temperatures of around 7 K.

For diamond the displacement threshold using electron-irradiation has been found to be about 150 keV [9] for ⟨100⟩ incidence whilst for SiC the Si displacement threshold for [0001] incidence is about 225 keV and the C displacement threshold is about 90 keV [10]. As an approximate measure, the average electron energy loss rate is about 1 kV μm^{-1}, so that atomic displacement occurred up to depths of 50–100 μm in the samples irradiated in the Philips TEM. The Renishaw systems, when adjusted for confocal operation, had a depth resolution of less than 10 μm and a lateral resolution of better than 1 μm. The electron beam spreading over such a depth can be estimated from widely used formulae (see [11] for example) as about 0.4 μm. This is not significant compared with the lateral resolution achieved. The most significant broadening effect came from drift and instability of the circular top-hat profile of the electron beam during irradiation. When drift had occurred, as in the case of longer (~1 h) exposures, it could be detected by loss of circular symmetry. In the worst cases of beam instability, using a high beam current, it introduced a broadening of ~5 μm. The ion beam was moved along a line on the sample with dwelling points for the implantations but as the beam was not shut off between the individual implantations, measurements of spreading were made perpendicular to this line. Confirmation of the lateral resolution under confocal operation was achieved by performing a line-scan across a cleavage edge of a sample and assuming a Gaussian profile to the beam. In addition one needs to take account of carrier diffusion within the sample under study and spreading of the electron beam in the specimen. Experimental evidence, such as that presented in figure 1, establishes that these effects did not contribute significantly to the broadening of the intensity distributions measured. The intensity profile in this figure is that of the neutral vacancy produced in diamond by electron-irradiation to a dose of 10^{20} e cm^{-2} at 175 keV to reduce the effect of vacancy migration. It represents a convolution of the electron beam profile, the laser beam profile, the vacancy migration and the carrier diffusion. These results are consistent with negligible beam spreading and a minority carrier diffusion length determined by EBIC experiments on 4H SiC as ~3 μm [12].

3. Experimental results

Our electron-irradiation experiments were designed to explore principally the influence of dose and dose rate on the long

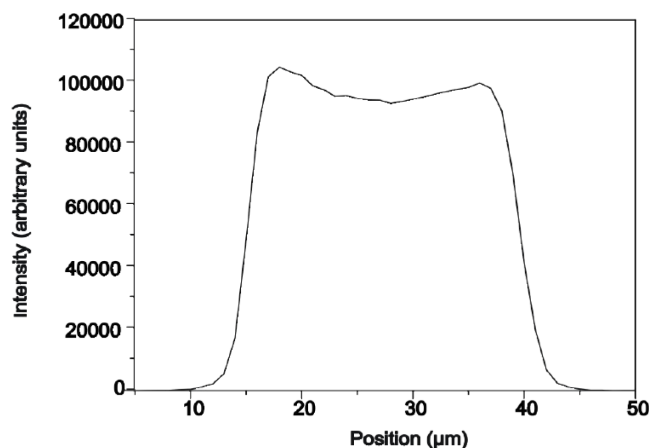

Figure 1. Neutral carbon vacancy intensity profile across a circular area of diamond irradiated at room temperature to a dose of 10^{20} e cm^{-2} at 175 keV.

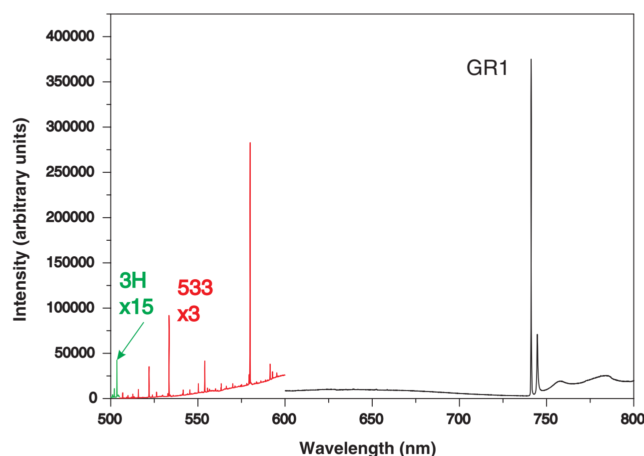

Figure 2. PL spectrum obtained at ~7 K with 488 nm excitation from the central region of an electron-irradiated low-N HPHT diamond single crystal. The electron dose was 5×10^{19} e cm^{-2} and the dose rate was 10^{16} e cm^{-2} s^{-1}. It is the highlighted ZPLs whose distribution is discussed in the text.

range migration of defects out of the irradiated regions of the purest and most perfect material available to us. The dose range explored was from 10^{16} to 10^{23} e cm^{-2}. The dose rate dependence was explored in two different ways. In one, the current was fixed and the irradiated area changed in size. This method facilitated a greater range of dose rates by a factor of 500 from 2.4×10^{15} to 1.2×10^{18} e cm^{-2} s^{-1}. In the second, the beam current was varied for a fixed irradiated area. This allowed a change in dose rate by a factor of 50. We shall start discussing results obtained on diamond samples and then present some of the results from 4H SiC. For the ion-implanted samples the H-implantations were for doses of 10^{18} cm^{-2} to 5×10^{20} e cm^{-2} and for the He-implantations they were for 5×10^{18} cm^{-2} to 5×10^{20} cm^{-2}.

3.1. Diamond samples

The general conclusion from the dose-rate experiments was that there was no marked effect on the tendency for migration of defects out of the irradiated area. There were spectral changes. The intensity of the neutral vacancy PL signal (GR1) decreased by a factor of two when the irradiated area decreased in diameter from 200 to 20 μm at a fixed beam current but was unchanged when the beam current was changed for a fixed area. Other zero phonon lines (ZPLs) in the spectra also decreased in intensity as the dose rate increased, for both types of experiment, but at varying rates. However, the forms of the intensity profiles for the centres that we shall concentrate on showed no significant variations.

Doses above about 10^{19} e cm^{-2} were found to have a strong effect on the intensity distributions. A typical spectrum obtained from the low-N HPHT sample after an electron dose of 5×10^{19} e cm^{-2} is shown in figure 2. Three ZPLs are identified. One of these is 3H PL (ZPL at 503.6 nm) that involves two close C interstitials [13]. Although its actual structure is not yet established it is a clear marker of C interstitial distribution. The single isolated interstitial in diamond has not been detected by PL [14]. The GR1 signal (ZPL at 741 nm) is used here as the marker of vacancy

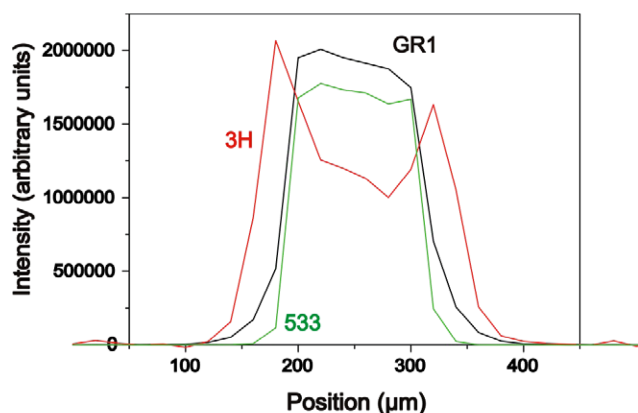

Figure 3. Intensity profiles obtained from a line-scan across the irradiated area for which a spectrum is shown in figure 2. The 3H intensity has been increased by 150× and the 533 nm intensity by 20× relative to the GR1 intensity.

distribution. The centre at 533.4 nm has a high energy local vibrational mode (LVM) at 184.4 meV, that broadens and shifts to lower energy in diamond enriched in ^{13}C, indicating that it is also C interstitial-related but its structure is unknown at present. It is selected here because it has been found in our experiments to be the most restricted to the region of irradiation itself.

Figure 3 shows the intensity line profiles across the irradiated region from which the spectrum in figure 2 was obtained. The intensities in figure 3 have been normalized to a similar peak value. The dose rate was relatively low, 10^{16} e cm^{-2} s^{-1}. In this case, the irradiated area was only about 115 μm in diameter so it is clear that outward migration had occurred. The 3H centre, which extends to a distance of about 100 μm outside the irradiated region, was generally found at the largest distances, but even the GR1 centre also extends well outside it. Only the 533 nm centre is fairly restricted in its extent. In addition, it will be noted that there is

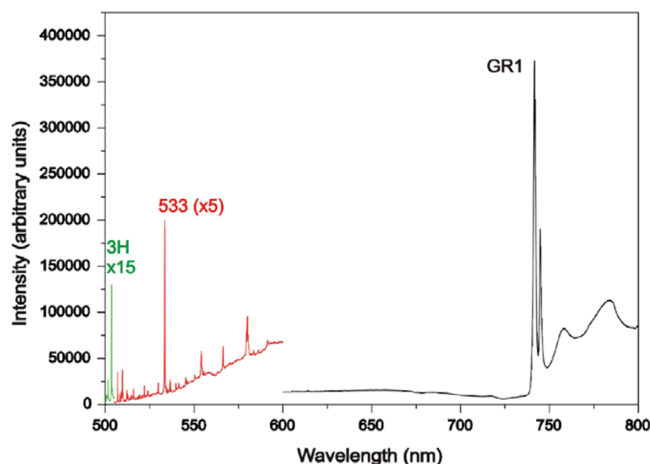

Figure 4. PL spectrum obtained at ~7 K with 488 nm excitation from the central region of an electron-irradiated natural IIA diamond single crystal. The electron beam was focused to a probe of a few micrometres diameter at an operating voltage of 600 keV and the dose was about 10^{23} e cm^{-2}.

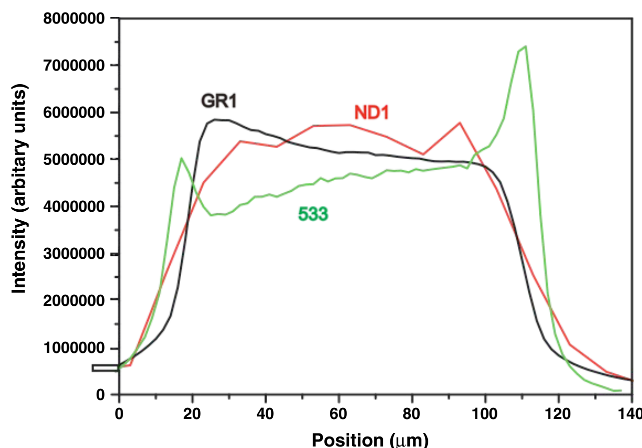

Figure 6. Intensity profiles obtained from a line-scan across the irradiated area of an ultra-high purity single crystal CVD diamond sample after a dose of 2×10^{20} e cm^{-2}. 325 nm (ND1) and 488 nm (GR1 and 580 nm) excitation at a temperature of about 7 K. The ND1 intensity has been increased by 500× and the 533 nm intensity by 200× relative to the GR1 intensity.

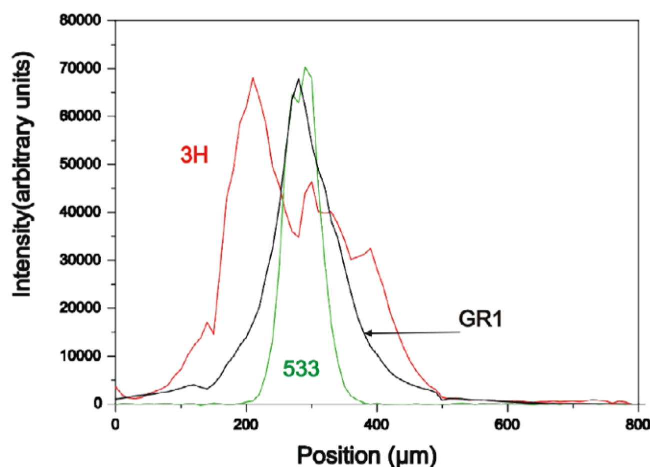

Figure 5. Intensity profiles obtained from a line-scan across the irradiated area for which a spectrum is shown in figure 4. The 3H intensity has been increased by 250× and the 533 nm intensity by 50× relative to the GR1 intensity.

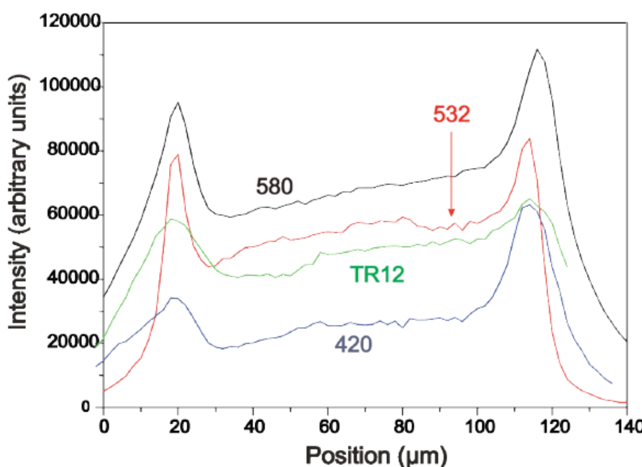

Figure 7. Intensity profiles obtained from the same area as that of figure 6 but with results obtained with both 325 nm (TR12 and 420 nm) and 488 nm (580 and 532 nm) excitations at a temperature of about 7 K. The 532 nm intensity has been increased by 5×, the TR12 by 2.5× and the 420 nm by 10× relative to the 580 nm intensity.

a maximum of 3H intensity near the periphery of the irradiated region with a local minimum at its centre.

As an extreme case the sample of natural IIA diamond was irradiated with a focused beam at 600 keV to a dose of about 10^{23} e cm^{-2}, producing the results shown in figures 4 and 5.

Figure 4 shows a particularly rich spectrum of ZPLs in the range 500–600 nm most of which are believed to be interstitial-related [1]. Figure 5 shows the spatial distribution of selected ZPLs with respect to the central (GR1 intensity maximum) region. Quite remarkable migration of defects over large distances has occurred. 3H luminescence exists up to more than 200 μm from the centre as does GR1 but to a lesser extent; the 533 nm emission is again mostly restricted to the irradiated region.

A more detailed study was made of the distribution of some of the shorter wavelength ZPLs with the ultrapure epitaxial single crystal CVD sample after irradiation to 2×10^{20} e cm^{-2}. 3H luminescence was not detected in this sample after irradiation but most of the other short wavelength lines of figure 4 were present. First, we illustrate in figure 6 intensity profiles for comparison with those in figures 3 and 5. Three rather similar profiles may be observed. The figure includes, in addition to the GR1 and 533 nm results, a profile for the negative vacancy (ND1-393 nm) obtained with 325 nm excitation. In this case the 533 nm intensity (LVM 184.4 meV) is enhanced at the periphery of the irradiated region, a quite common phenomenon at this dose for some of the other ZPLs in this material, as illustrated in figure 7, which was also prepared from results obtained at both 488 and 325 nm laser excitations. It is notable that most of these ZPLs have

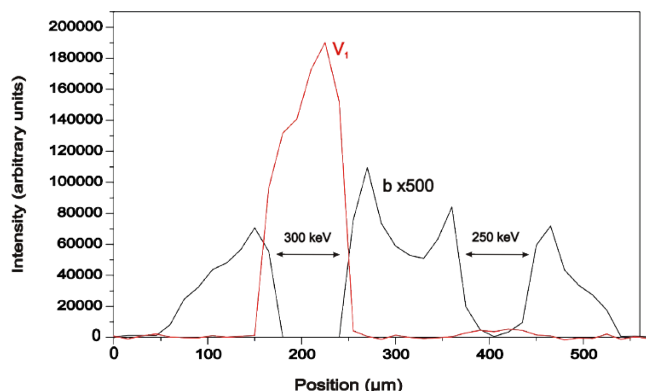

Figure 8. Intensity profiles across two electron-irradiated circular areas, each of 100 μm diameter and 200 μm apart, obtained with 488 nm excitation at a temperature of about 7 K. Each had a dose of 10^{20} e cm^{-2} but at different electron energies; left—300 keV, right—250 keV. As the b-line appeared by second-order diffraction of an up-converted first-order line it was rather weak and its intensity has been increased by 500× in comparison with the V_1 line.

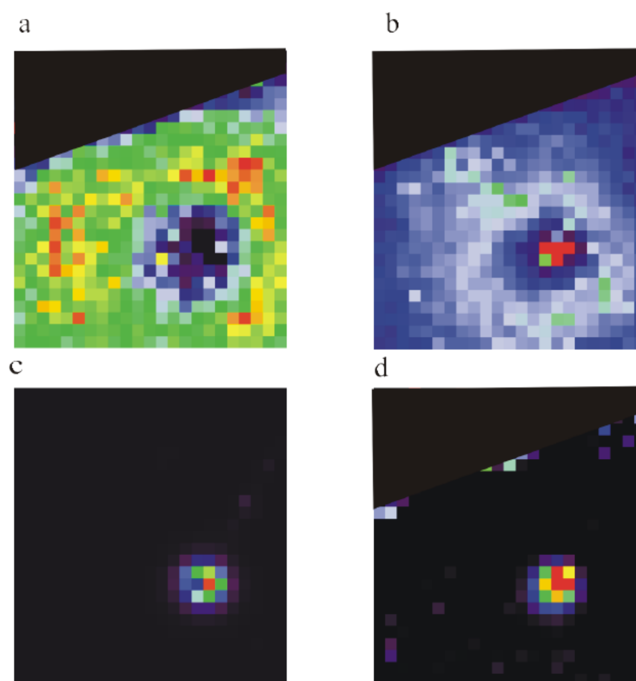

Figure 9. Integrated intensity and peak-position maps for a 4H SiC sample electron-irradiated to a dose of 10^{23} e cm^{-2} with a focused electron beam. The sample was N-doped to about 5×10^{15} cm^{-3} and the accelerating voltage was 300 kV. The spectral data were collected with 325 nm excitation at a sample temperature of about 7 K. The black regions in the top left-hand corners are regions off the edge of the sample. The pixel size is 5 μm. The maps are as follows: (a) c-alphabet line intensity; (b) b-alphabet line intensity; (c) V_1 intensity; (d) V_1 peak position. The electron beam was incident at the red region in (b) or (d). Low to high intensity (or short to long wavelength) is represented by the sequence black-dark blue-light blue-green-yellow-red (light to dark in the printed version).

associated with them high energy LVMs as follows: 420 nm—202 meV; TR12 (469 nm)—197 meV; 580 nm—237 meV. The association of such high energy LVMs with these centres in such pure material is good evidence of the interstitial nature of the defects. Note that the 532 nm emission is distinct from the 533 nm emission.

Equivalent experiments to those described above were also performed on the B-doped diamond in table 1 with B in the range 2–8 ppm, depending on the growth sector. In this case the only ZPL in common with the results above was GR1 and it was considerably more restricted to the irradiated region for this material.

3.2. 4H–SiC samples

The range of samples for which we present results is given in table 2. For this material we will concentrate on the so-called alphabet lines [15] that are believed to originate from C interstitials [16] and the Si vacancy-related PL known as V_1 (861 nm) [17] in order to make comparison with the results from diamond.

A first example of the alphabet and V_1 intensity distributions, obtained with 488 nm excitation is given in figure 8. This compares their intensity profiles across two electron-irradiated areas, one irradiated at an energy of 300 keV, the other at 250 keV, both at doses of 10^{20} e cm^{-2}. Examples of spectra similar to that from which these results were generated can be found in [2]. The sample was p-type 4.8×10^{15} cm^{-3} and revealed no detectable nitrogen bound exciton PL using 325 nm excitation. 300 keV is above the Si displacement threshold in 4H SiC and 250 keV is near the threshold, so that the V_1 intensity is very weak in the latter region. It can be seen that the Si vacancies are restricted to the irradiated area while the alphabet b-line extends to considerable distances outside it. The alphabet lines in this spectrum are relatively weak because they appear in the spectrum as second-order diffraction from the grating used by up-conversion of first-order lines. With 325 nm excitation (above band-gap) their intensities were very much greater and the lines also existed in the irradiated region itself (see [2], for example, or figure 10 below). Because PL is a competitive process, the high intensity of the V_1 emission in the irradiated region together with that of a number of other centres with 488 nm excitation (see [2]) robs the rather weak second-order alphabet lines of excitation. It should be noted that the 488 nm spectrum from the 300 keV spectra, from which figure 8 was derived, contained a ZPL at 737.1 nm that we have shown to anneal out at 250 °C.

As with the diamond samples, a more extreme effect was produced using a focused electron beam at a dose of 10^{23} e cm^{-2}, now using 300 keV electrons. This is illustrated in figure 9. The two-dimensional rainbow coloured intensity maps (grey scale in the printed version) illustrate: (a) c-alphabet line; (b) b-alphabet line; (c) V_1. (d) is a map of the peak wavelength of V_1, black indicating its normal wavelength, red indicating its red-shift near the position of irradiation. The peak shift is associated with considerable peak broadening. The contrast between the outwards migration indicated by the alphabet lines and that of the Si vacancy is particularly strong. The apparent increase of b-line intensity at the beam position is not a real effect but is caused by part of the vibronic structure of the Si-vacancy spectrum.

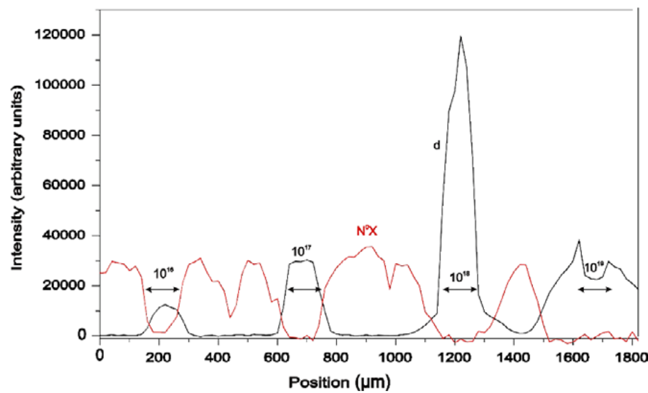

Figure 10. Intensity profiles of bound exciton PL (N^0X) and of the d-line across four 300 keV circular electron-irradiated areas of 100 μm diameter showing the effect of electron dose. The doses are as given at the four different locations (in units of e cm^{-2}); 488 nm excitation at about 7 K.

The PL results in figure 10 were obtained with 325 nm laser excitation of a sample that was p-type 2×10^{14} cm^{-3} but with stronger N- than Al-bound-exciton emission. Four electron irradiations were performed at 300 keV over circular areas, each 100 μm in diameter and displaced from each other along a line by a distance of 500 μm, starting at a dose of 10^{16} e cm^{-2} and increasing by factors of ten up to a dose of 10^{19} e cm^{-2}. The spectral range covered by the line-scan was from 370 to 470 nm and the intensity profiles shown in the figure were generated from this data set. Two spectral features have been selected, that of the N-bound exciton luminescence (N^0X) and the d alphabet line. It is clear from this figure that as the dose increased the area covered by the d luminescence also increased and that of the bound exciton luminescence decreased. The dip in bound exciton luminescence between the 10^{16} and the 10^{17} e cm^{-2} regions is a random fluctuation. For the two lowest doses the d luminescence was restricted to the irradiated region. The integrated intensity of the d-line increased progressively up to a dose of 10^{18} e cm^{-2} but at this latter dose the first signs of outward migration appeared as shoulders to the intensity distribution. For the dose of 10^{19} e cm^{-2} a major change had occurred with a large drop in maximum intensity and an actual dip in the intensity in the irradiated region relative to the intensity just outside it. This was accompanied by strong outwards migration of the defect and quenching of N^0X PL over an equivalent distance The maximum of the intensity of the d-profile at the periphery of the irradiated region is similar to that remarked on above in the context of diamond interstitial-related centres.

Very similar results were obtained from all the rather pure materials listed in table 2, both n- and p-type. This situation was not anticipated but it may be explained by the shift of the Fermi level to a mid-gap position after high electron doses applied to lightly doped material. This change of Fermi level could be monitored in the case of n-type material by measuring the wavelength or intensity of the longitudinal optic phonon line. Initially weak, because of plasmon interaction with the free electrons, it became much stronger on irradiation and shifted to the wavenumber of semi-insulating or p-doped material. However, a completely different situation was encountered on electron-irradiation of highly N-doped material ($n \geqslant 10^{18}$ e cm^{-3}) or for rather impure substrate material. Only very limited outward migration of any electron irradiation-induced defect occurred for these presumably because of defect-trapping by the impurities.

The results obtained from the ion-implanted 4H SiC samples were rather similar to those obtained by electron-irradiation [18]. Si-vacancy PL was restricted to locations close to the position of the implant and alphabet line emission extended well outside this region and to greater distances with increase of dose. There was one important difference. The extent of the outward migration was significantly lower than that observed for high electron doses and ranged from 5 μm to 25 μm as the ion dose increased.

4. Discussion

The foregoing experiments have produced a number of surprising results that we now discuss. The key conclusions that can be deduced from the experiments are that the outwards migration is mainly controlled by dose and is not appreciably affected by dose rate or specimen temperature during irradiation. The effect is still present, but reduced, for ion-implantation of H or He. The different intensity profiles for different ZPLs reveal that vacancies migrate less than interstitials in diamond and Si vacancies migrate less than C interstitials in 4H SiC. Reasonable values for the migration energies of these defects are known, ~1.6 eV for C interstitial migration in diamond ~2.3 eV for the vacancy [19], ~1 eV for the C interstitial in SiC and ~2.5 eV for the Si vacancy [20]. It follows that the lower the migration energy the greater the tendency for outward migration as demonstrated by the experimental results presented here.

In addition to atomic displacement, the irradiations create a great deal of ionization. For electron-irradiation the ratio of ionization to displacement is considerably higher than for ions [21]. The ionization creates carriers that can be trapped by the defects facilitating their migration and the carrier recombination creates light that can be subsequently absorbed by the material. Since, given their band-gap energies, the recombination of electrons and holes provides sufficient energy to cause migration of the relevant interstitials and vacancies in these materials, the key issue is to understand how the defect migration takes place over such large distances. There are several possible contributing factors. These include electric fields, stress fields and absorption of energy by the defects from the light emission but exclude thermal effects because the dose rate was not a significant factor and there is direct evidence that any temperature rise was small.

That electric fields exist near the irradiated regions is evident from the band-bending caused by the mid-gap pinning of the Fermi level for which we have direct evidence as mentioned above. In addition, on studying the irradiated diamond samples in a scanning electron microscope after irradiation, strongly enhanced secondary electron emission occurred from the irradiated regions and this effect persists for several weeks after the time of irradiation. This effect is

caused by trapped negative charge left over from the excess of electrons introduced during irradiation. It is likely that a similar effect occurs, though to a lesser extent, in the 4H SiC where the material has become semi-insulating because of Fermi level pinning.

There is also clear evidence of stress associated with the irradiated regions. Not infrequently, spallation of material occurred from highly dosed regions of 4H SiC some weeks after the time of irradiation (see [18] for examples). It is well known that dilatational effects associated with interstitial atoms in diamond generate compressive stresses [22]. Attempts were made to measure this stress directly by Raman spectroscopy without obtaining unambiguous results. The Raman line peak positions along line-scans through the irradiated regions failed to show a detectable effect with a sensitivity of 0.5 cm^{-1} in either diamond or SiC specimens but they have not yet been performed on the regions of highest dose (because spallation occurred first). However, the stress-sensitivity to stress is low compared with that of vacancy-related PL centres. We have presented evidence that considerable broadening of the Si-vacancy PL occurs in the highly irradiated regions of 4H SiC accompanied by a red-shift of the ZPL maximum (figure 9(d)). This effect can be caused by both stress and electric fields. The situation that emerges from this evidence is one in which the carriers are driven out of the irradiated region by these fields. In view of the fact that the band-bending will occur in opposite senses in the p- and n-doped samples but the migration of defects is similar in both indicates that it is either, or both, the trapped negative charge or the stress fields that are the origin of the effect. At this point it should be noted that similar outward migration was neither observed in highly n-doped 4H SiC substrate material nor in the B-doped diamond. Here the material remained conducting after irradiation so that charge retention would not have occurred and any band-bending would have been greatly reduced. In addition, the higher impurity level would limit the carrier mobility. In contrast, very long carrier-collection distances, greater than 150 μm, have been measured in very pure diamond under the influence of electric fields [23].

Quite apart from the probable contribution of electric and stress fields to the outwards migration of defects, we also need to consider the possible contribution of the light emitted during irradiation. This will have a relatively broad spectrum, involving both near band-gap energy photons as well as defect-related emission. As 4H SiC is an indirect band-gap material, photon absorption is relatively weak so that even for band-gap emission the absorption length is $\sim$7 μm and this increased to $\sim$80 μm at 488 nm so that defects migrating from the irradiated region can absorb light and continue migrating by one or more of the mechanisms that have been proposed [24]. There is insufficient evidence at present to decide which of these is most likely to have occurred. Similar considerations apply to the case of diamond except that for this material all the results are for photons of below band-gap energy. There is direct evidence of self-absorption by vacancies and interstitials in the PL spectra obtained as can be seen in figure 4.

Our association of the alphabet lines with C interstitials in 4H SiC calls for some discussion. Previous theoretical work [25] has identified the a–d alphabet lines with nearest-neighbour C antisite–Si antisite pairs and this conclusion is supported quite widely [26]. A related work describes how C interstitials can be converted to C/Si nearest-neighbour antisite pairs by a process with an energy barrier of 0.6 eV that involves charge neutralization by electrons. There is no known PL signature of Si interstitials at present. We conclude that the C interstitials migrate outwards by some combination of the mechanisms discussed and at some point in this process become converted to C/Si antisite pairs [27]. As mentioned previously, the 3H centre in diamond has been shown to involve C interstitials but it is a complex defect, unlikely to migrate itself, so a conversion process must also occur at distant points.

Unfortunately, there are too many unknown factors at present to proceed with any numerical analysis. Available data permit estimates of the vacancy and electron–hole production but the interstitial atoms form several complexes as well as being lost to sinks so that the results for the 3H luminescence in diamond and for the alphabet luminescence in 4H SiC cannot be put on a quantitative basis. A low-N HPHT diamond sample, provided by Dr M Newton, with an epr-calibrated vacancy concentration of 1 part/million was studied by PL, and by comparison of relative intensities we deduce that an ultrapure single crystal CVD diamond sample after a 300 keV dose of 10^{19} e cm^{-2} had a vacancy concentration of about this amount. According to [28] a dose of 2×10^{18} e cm^{-2} of 1.9 MeV electrons in a 2 mm thick sample produces a vacancy concentration of 10 ppm (or 10^{18} cm^{-3}) which, even given the uncertainties involved in our estimated vacancy concentration, implies a considerably lower vacancy production rate for the lower energy electrons. By way of comparison, an upper limit to the electron–hole pair production can be estimated as follows. On the basis that it takes approximately three times the band-gap energy to create an electron–hole pair, or 16.5 eV for diamond, and that the high energy electron loses approximately 1 keV μm^{-1} of path length, we deduce an e/h production rate of 60 μm^{-1}. For a 50 μm generation depth of 300 keV electrons and a dose of 2.5×10^{19} e cm^{-2} this gives a maximum pair density of 3×10^{22} cm^{-3}.

A possible reason for the large drop in alphabet line intensity at a dose of 10^{19} e cm^{-2} that may be seen in figure 10 is the creation of sufficient deep centres that rob the alphabet lines of excitation. Such an effect has been reported for damage centres in electron-irradiated cubic BN [29]. The smaller effect for the interstitial-related centres in the results from diamond may just be the consequence of competition for excitation in the central region where the vacancy density is high.

5. Summary and conclusions

Defects created by electron-irradiation or ion-implantation of diamond or 4H SiC can migrate over distances that are much greater than is generally realized. C interstitials in both materials can migrate over distances greater than 100 μm in diamond and 4H SiC but vacancies in diamond and Si vacancies in 4H SiC migrate over shorter distances. The migration energy appears to be the factor controlling the differences. The effect becomes important for electron doses

above 10^{19} e cm^{-2} and is considerably greater for 300 keV electrons than for H or He ions. It is concluded that the process is driven by one or more consequences of the ionization that occurs during irradiation or implantation. Carriers, thereby created, can be driven out of the irradiated or implanted region by electric or stress fields and are captured by the migrating defects. The defects may also absorb light that is a consequence of the decay of the ionization. The general picture that emerges is one of self-interstitials moving rather freely under electron-irradiation and it is likely that this effect may operate in other semiconductors.

Acknowledgments

The authors wish to acknowledge access to the HREM at the National Center for electron Microscopy at Berkeley CA and the expert assistance of Cheng Yu Song for high voltage irradiations. We also thank Dr M Newton (University of Warwick) for the diamond vacancy calibration sample and Ninhua Peng for the ion-implantations. Gunther Wagner (IKZ), Peter Friedrichs (SiCrystal), Peder Bergman (Linköping) and Fracesco la Via (ST Catania) kindly provided 4H SiC samples and Jim Butler (NRL), DTC and Element six diamond samples. We thank DTC, the UK Engineering and Physical Science Research Council and the Leverhulme Trust for partial support of this work.

References

[1] Steeds J W, Charles S, Davis T J, Gilmore A, Hayes J, Pickard D and Butler J E 1999 *Diamond Relat. Mater.* **8** 94
[2] Steeds J W, Evans G A, Danks L R, Furkert S, Voegeli W, Ismail M M and Carosella F 2002 *Diamond Relat. Mater.* **11** 1923
[3] Starodubtsev S V, Niyazova O R and Kaneev M A 1967 *Sov. Phys.—Solid State* **9** 679
[4] Ferreira Lima C A and Howie A 1976 *Phil. Mag.* **34** 1057
[5] Stevens Kalceff M A and Phillips M R 1995 *Phys. Rev.* B **52** 3122
[6] Jim Y G and Chang K J 2001 *Phys. Rev. Lett.* **86** 1793
[7] Popovici G, Wilson R G, Sung T, Prelas M A and Khasawinah S 1995 *J. Appl. Phys.* **77** 5103
[8] Newton M E, Campbell B A, Twitchen D J, Baker J M and Anthony T R 2002 *Diamond Relat. Mater.* **11** 618
[9] Wotherspoon A, Steeds J W, Coleman P, Wolverson D, Davies J, Lawson S and Butler J 2002 *Diamond Relat. Mater.* **11** 692
[10] Steeds J W, Carosella F, Evans G A, Ismail M M, Danks L R and Voegeli W 2001 *Mater. Sci. Forum* **353–356** 381
[11] Yacobi B G and Holt D B 1990 *Cathodoluminescence Microscopy of Inorganic Solids* (New York: Plenum)
[12] Diaz-Guerra C and Piqueras J 2004 *J. Phys.: Condens. Matter* **16** S217
[13] Steeds J W, Davis T J, Charles S J, Hayes J M and Butler J E 1999 *Diamond Relat. Mater.* **8** 1847
[14] Davies G, Smith H and Kanda H 2000 *Phys. Rev.* B **62** 1528
[15] Egilsson T, Henry A, Ivanov I G, Lindström J L and Janzén E 1999 *Phys. Rev.* B **59** 8008
[16] Eberlein T A G, Jones R Öberg S and Briddon P R 2006 *Phys. Rev.* B **74** 144106
[17] Sörman E, Son N T, Chen W M, Kordina O, Hallin C and Janzén E 2000 *Phys. Rev.* B **61** 2613
[18] Steeds J W, Peng N and Sullivan W 2009 *Mater. Sci. Forum* **615–617** 409
[19] Watkins G D 2001 *Phys. Status Solidi* a **186** 167
[20] Bockstedte M, Mattausch A and Ponkratov O 2004 *Phys. Rev.* B **69** 235202
[21] Campbell B and Mainwood A 2000 *Phys. Status Solidi* a **181** 99
[22] Goss J P, Jones R and Briddon P R 2001 *Phys. Rev.* B **65** 035203
[23] Tapper R J 2000 *Rep. Prog. Phys.* **63** 1273
[24] Corbett J W 1966 *Electron Radiation Damage in Semiconductors and Metals* (New York: Academic)
[25] Eberlein T A G, Fall C J, Jones R, Briddon P R and Öberg S 2002 *Phys. Rev.* B **65** 184108
[26] Gali A, Deák P, Rauls E, Son N T, Ivanov I G, Carlsson F H C, Janzén E and Choyke W J 2003 *Phys. Rev.* B **67** 155203
[27] Steeds J W 2009 *Mater. Sci. Forum* **600–603** 437
[28] Lawson S C, Fisher D, Hunt D C and Newton M E 1998 *J. Phys.: Condens. Matter* **10** 6171
[29] Shishonok E M and Steeds J W 2002 *Diamond Relat. Mater.* **11** 1174